

Cross-Image Contrastive Decoding: Precise, Lossless Suppression of Language Priors in Large Vision-Language Models

Jianfei Zhao^{1,2}, Feng Zhang¹, Xin Sun¹, Chong Feng^{1,3,*},

¹School of Computer Science and Technology, Beijing Institute of Technology, Beijing, China,

²Zhongguancun Academy, Beijing, China,

³Southeast Academy of Information Technology, Beijing Institute of Technology, Fujian, China,

Abstract

Language priors are a major cause of hallucinations in Large Vision-Language Models (LVLMs), often leading to text that is linguistically plausible but visually inconsistent. Recent work explores contrastive decoding as a training-free solution, but these methods typically construct negative contexts from the original image, resulting in visual information loss and distorted distribution. Motivated by the observation that language priors stem from the LLM backbone and remain consistent across images, we propose Cross-Images Contrastive Decoding (CICD), a simple yet effective training-free method that uses different images to construct negative contexts. We further analyze the cross-image behavior of language priors and introduce a distinction between essential priors (supporting fluency) and detrimental priors (causing hallucinations). By selectively preserving essential priors and suppressing detrimental ones, our method reduces hallucinations while maintaining coherent and fluent language generation. Experiments on 4 benchmarks and 6 LVLMs across three model families confirm the effectiveness and generalizability of CICD, especially in image captioning, where language priors are particularly pronounced. Code will be released once accepted.

1 Introduction

Recent advances in Large Language Models (LLMs) (Brown et al., 2020; Touvron et al., 2023; Chiang et al., 2023; Bai et al., 2023a) have opened promising pathways toward Artificial General Intelligence (AGI). Building on these developments, numerous studies (Liu et al., 2023; Dai et al., 2023; Bai et al., 2023b, 2025) have extended LLMs by integrating visual inputs, giving rise to Large Vision-Language Models (LVLMs) capable of understanding visual content. They are capable of addressing

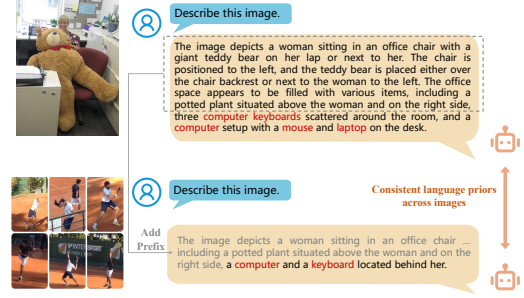


Figure 1: A case of language prior. Adding the same prefix when captioning another image will lead to the same language priors. The model used is LLaVA-1.5.

a broad spectrum of vision-language tasks, such as image captioning (Jing et al., 2024; Rohrbach et al., 2018; Ye et al., 2025; Chen et al., 2025), visual question answering (VQA) (Lovenia et al., 2024; Li et al., 2023b; Yu et al., 2024), and visual grounding (Rasheed et al., 2024; You et al., 2024; Lu et al., 2024).

Despite impressive capabilities, LVLMs remain susceptible to hallucinations (Li et al., 2023c; Wang et al., 2023), often generating text that contradicts the visual input. These hallucinations stem from various sources, with language priors (Chen et al., 2025; Leng et al., 2024; Wang et al., 2024c; Zhu et al., 2024b) being the most fundamental underlying cause. Specifically, since LVLMs are built upon LLMs, they inherently inherit the linguistic knowledge encoded in the LLMs. As a result, their outputs are influenced not only by visual evidence but also by pre-learned language patterns. This often leads to a tendency to rely on memorized linguistic associations when responding to user queries. For instance, when describing an office scene, an LVLM may erroneously mention a "computer" even if no such object is present in the image.

Methods for mitigating language priors in LVLMs can generally be classified into two cat-

*Corresponding Author: fengchong@bit.edu.cn

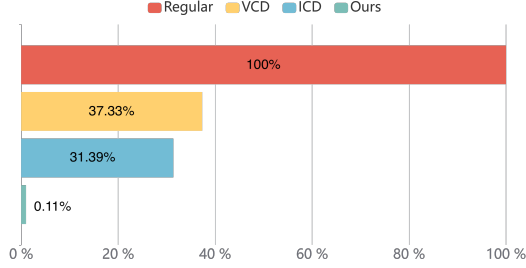


Figure 2: The overlap ratio of image-related words between responses generated from negative contexts and those from regular inputs. Both VCD and ICD exhibit over 30% overlap, indicating that their negative contexts retain a considerable amount of essential visual information. In contrast, our method results in a nearly negligible overlap. The detailed analysis methodology can be found in Appendix. D.

egories. The first involves constructing specialized training datasets to reduce the model’s dependence on linguistic biases (Zhibo et al., 2023; Wu et al., 2022; Chen et al., 2025), though such approaches often incur substantial training costs. Another line of work explores plug-and-play, training-free methods, which are also the focus of our study. Among them, many recent studies adopt contrastive decoding (Li et al., 2023a), which constructs negative contexts to reveal and suppress language priors. Some approaches directly perturb the input image (Leng et al., 2024; Wang et al., 2024c) to alter the visual context, while others enhance the visual features extracted from the original image (Zhu et al., 2024b; Zhang et al., 2025). These methods typically compute the difference between the logit distributions obtained from the original and perturbed (i.e., negative) contexts to reduce the model’s reliance on language priors. Overall, following the paradigm introduced in VCD (Leng et al., 2024), these methods routinely perturb the original inputs to generate negative contexts. However, this prevailing design choice raises a critical question: **Is perturbing the original context to construct negative contexts truly the most effective strategy for inducing and mitigating language priors?**

We argue that the answer is unequivocally **negative**. Constructing negative contexts based on the original inputs can lead to two main issues: (1) *Visual information loss*, where the negative context retains partial visual information, which may be degraded during contrastive decoding. As shown in Fig. 2, compared to regular responses, those generated from negative contexts retain over 30% of the essential visual information, which is subse-



Figure 3: Essential priors (left) and detrimental priors (right). We randomly select 500 images from the MSCOCO dataset and visualize LLaVA-1.5’s output by the t-SNE algorithm (van der Maaten and Hinton, 2008). *w/ Image* represents regular outputs. *w/o Image* represents the outputs after removing the input image. *w/ Neg. Image* represents replacing the input image by the most dissimilar image in the dataset retrieved by CLIP (Radford et al., 2021).

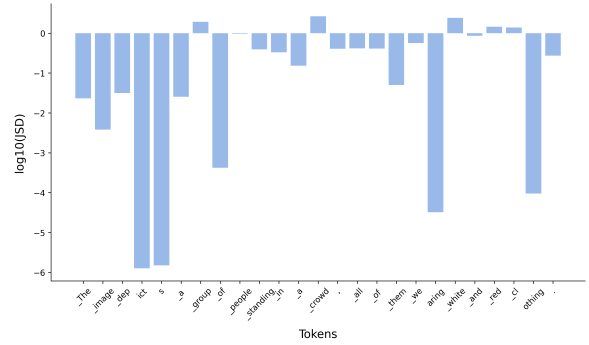


Figure 4: A case of JS divergence between the logit distributions of two images.

quently weakened during the contrastive decoding process. (2) *Distorted distribution*, where perturbing the model’s input to induce priors may disrupt its internal representations, ultimately resulting in a distorted logit distribution. This analysis raises an important question: **How should negative contexts be constructed to avoid the above issue?**

In fact, **simply taking a different image to construct negative context is sufficient**. This insight is based on the thought that the language priors guiding step-wise token generation in LVLMs originate from the LLM backbone and are largely independent of the input image. As shown in Fig. 1, LVLm produces highly consistent outputs when given completely different images but the same prefix, which strongly supports our hypothesis. Building on this, we propose Cross-Images Contrastive Decoding (CICD), a simple yet effective method for suppressing language priors in LVLMs. Instead of perturbing the original inputs, CICD constructs the negative context using a different image

that shares the same language priors. Our method avoids the two key issues present in previous approaches. Since the overlap between the original and the new image is limited, our approach avoids introducing critical visual information into the negative context. As shown in Fig. 2, only a negligible amount (approximately 0.11%) of essential visual information is retained in our negative context. Moreover, it enables the model to reveal intrinsic priors, maintaining the model’s natural inference process without injecting external bias. The formal analysis of our method is presented in Sec. 3.2.

Focusing on language priors, we further explore **whether all such priors should be strictly eliminated**. The answer is intuitively **negative**. Language priors can be divided into two categories: (1) *Essential Priors*, which are necessary for maintaining textual fluency, and (2) *Detrimental Priors*, which introduce information unrelated to the visual input. Clearly, only the detrimental priors should be removed. This raises a critical question: **How can we accurately distinguish between the two and selectively eliminate only the detrimental ones?** As shown in Fig. 3, essential priors exhibit high consistency across different images, whereas detrimental priors show substantial divergence when generating image-related content. Based on this observation, we propose to distinguish essential from detrimental priors using cross-image consistency, as illustrated in Fig. 4. Specifically, we compute the Jensen–Shannon (JS) divergence between the logit distributions of different visual contexts, and apply a stable threshold to identify essential priors that should be retained.

Extensive experiments on 4 widely used benchmarks and 6 LVLMS across three model families demonstrate the effectiveness and generalizability of our method. By suppressing language priors, CICD consistently reduces hallucinations and achieves state-of-the-art performance across all benchmarks. The improvement is particularly pronounced in the image captioning task, which tends to suffer more from language priors due to its longer textual outputs.

In summary, our main contributions are as follows:

- We analyze existing contrastive decoding methods in depth and reveal their limitations stemming from reliance on the original image. To address this, we verify the consistency of language priors across images and propose a

stable approach to distinguish essential priors from detrimental ones.

- Based on this analysis, we propose CICD (Cross-Images Contrastive Decoding), which leverages retrieved images to induce language priors while selectively preserving essential priors during the mitigation process.
- Extensive experiments on multiple benchmarks and LVLMS demonstrate the superiority of our method in alleviating language priors, particularly in the image captioning task.

2 Related Work

Due to space limitations, we provide a brief overview here. A more detailed discussion of related work can be found in Appendix A.

2.1 Hallucination in LVLMS

Hallucinations in LVLMS primarily concern cross-modal consistency (Li et al., 2023c; Wang et al., 2023), which requires that the generated content remains faithful to the visual input. Among the various causes of hallucination, language priors (Zhibo et al., 2023; Wu et al., 2022) are the most fundamental. These priors originate from the LLM’s pretraining corpus and guide generation based on learned language patterns, which can produce fluent yet visually inconsistent outputs. Several approaches (Chen et al., 2025; Liu et al., 2024a; Gungal et al., 2024) attempt to mitigate language priors by constructing specialized training datasets, but these methods often incur significant additional training costs. Alternatively, recent training-free methods have explored contrastive decoding (Li et al., 2023a; Chuang et al., 2024), typically constructing negative contexts based on the original image (Leng et al., 2024; Wang et al., 2024c; Zhu et al., 2024b; Zhang et al., 2025) in an attempt to elicit and suppress language priors.

In this work, we identify critical limitations of these approaches that stem from their reliance on modifying the original image. Specifically, such modifications may lead to visual information loss and distorted distribution. We further conduct an in-depth analysis of the cross-image consistency of language priors and, based on this insight, propose CICD. Additionally, we introduce a method for distinguishing between essential priors and detrimental priors, enabling fine-grained and precise

mitigation of language priors in LVLMs.

3 Preliminary

3.1 Contrastive Decoding

LVLMs take as input a concatenation of vision tokens from a vision encoder and an encoded text prompt. After forward propagation, the model projects the output into a logit distribution to compute conditional probabilities and generate responses in an autoregressive manner:

$$y_t \sim p_\theta(y_t | v, x, y_{<t}) \\ = \text{softmax}[\text{logit}_\theta(y_t | v, x, y_{<t})] \quad (1)$$

Here, v and x represent the visual and textual inputs, respectively. logit_θ represents the logit distribution formulated by the model with parameters θ .

Since LVLMs adopt pretrained LLMs as their backbone, they inherently inherit language priors independent of the visual input. As a result, tokens ranked higher in the output distribution logit_θ may appear semantically plausible but can be objectively inconsistent with the visual evidence. This constitutes a fundamental cause of hallucinations. A commonly used approach to mitigate such priors is contrastive decoding (Li et al., 2023a; Leng et al., 2024), which modifies the original image to construct a native visual context that elicits language priors. These priors are then suppressed by subtracting the logit distribution derived from the native context from that of the original context.

$$\text{logit}_{\text{CD}}(y_t | v, x, y_{<t}) \\ = (1 + \alpha) \text{logit}_\theta(y_t | v, x, y_{<t}) - \alpha \text{logit}_N \quad (2)$$

Here, logit_N denotes the logit distribution obtained from the native context, and logit_{CD} represents the final distribution used for next-token prediction.

3.2 Formal Analysis

The core component of contrastive decoding lies in the construction of the native context. Our preliminary investigation reveals that existing methods, which modify the original image, introduce several limitations (see Sec.1). Further observations and analysis show that language priors are inherent characteristics of LVLMs and remain consistent across different images, as illustrated in Fig.1. This insight leads to a natural alternative, where the native context is constructed using an image distinct

from the original. Under this design, Eq. 2 is refined as:

$$\text{logit}_{\text{CD}}(y_t | v, x, y_{<t}) \\ = (1 + \alpha) \text{logit}_\theta(y_t | v, x, y_{<t}) \\ - \alpha \text{logit}_\theta(y_t | v', x, y_{<t}) \quad (3)$$

where v' is a different image from v . We further provide a formal analysis of the effectiveness of this approach.

Most existing methods employ sampling decoding, where a token is randomly selected according to the logit distribution. We define the set of plausible tokens under a given logit distribution as $S = V \cup T$, where V represents tokens related to visual content, and T represents tokens unrelated to the image, *i.e.*, those driven by language priors. The negative context constructed by a different image yields a new logit distribution, whose plausible token set is $S' = V' \cup T$, given that language priors remain unchanged across images. The contrastive decoding operation can thus be interpreted as subtracting one plausible token set from another:

$$S - S' = (V \cup T) - (V' \cup T) = V \text{ if } V' \cap V = \emptyset \quad (4)$$

In other words, this subtraction removes all language priors that are unrelated to the visual input. This approach achieves three objectives simultaneously: (1) retention of all essential visual information, (2) precise elimination of language priors, and (3) compatibility with the input distribution expected by LVLMs.

4 Method

Leveraging the cross-image consistency of language priors, we propose CICD (Cross-Images Contrastive Decoding), which effectively mitigates language priors while preventing visual information loss. In addition, we retain essential linguistic priors to ensure fluent and natural generation. As illustrated in Fig. 5, CICD comprises three key steps: (1) retrieving a distinct image, (2) identifying detrimental language priors, and (3) removing these priors through contrastive decoding.

4.1 Image Retrieval

As discussed earlier, it is essential to select an image with limited information that overlaps with the input image. Since visual features are extracted by the vision encoder, a natural strategy is to measure the similarity between two images using the

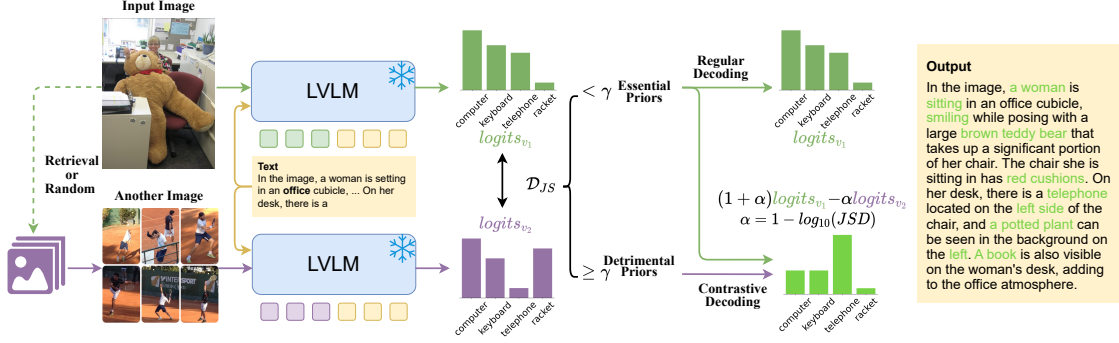


Figure 5: The diagram of our method. We input the target image and a distinct image into the LVLM separately. During the step-by-step generation of the response, we compute the Jensen-Shannon (JS) divergence between the two logit distributions at each step to distinguish essential priors from detrimental ones. For detrimental priors, we apply contrastive decoding to suppress harmful language biases, while regular decoding is used for essential priors.

encoder itself to estimate their overlap. In other words, the image with the lowest similarity to the input image is selected as the reference. To ensure better generalizability, we adopt the pretrained CLIP model (Radford et al., 2021) as the retriever. All images in the dataset are vectorized in advance, and during inference, the image with the lowest cosine similarity to the input is retrieved as the contrastive image.

Although vector retrieval is relatively efficient given the computational cost of LVLMs, practical deployment still requires loading an additional retriever and maintaining a vector database. As illustrated in Fig.1, we observe that **language priors primarily manifest in content words** such as objects, attributes, and relationships. These visual elements tend to **exhibit minimal overlap across natural images**. Therefore, randomly selecting an image can serve as an effective and lightweight alternative for practical applications. We provide further discussion in Appendix.C.2. Note that, to ensure reproducibility, we adopt the retrieval-based strategy for consistent and deterministic image selection throughout all experiments.

4.2 Identifying Detrimental Priors

Although language priors may cause LVLMs to generate hallucinated content, they remain essential for producing fluent and coherent text. To address this, we categorize language priors into two types: essential priors and detrimental priors, with only the latter requiring elimination. Essential priors are defined as purely linguistic patterns that are entirely independent of visual input. As discussed in Sec. 1, the logit distributions associated with

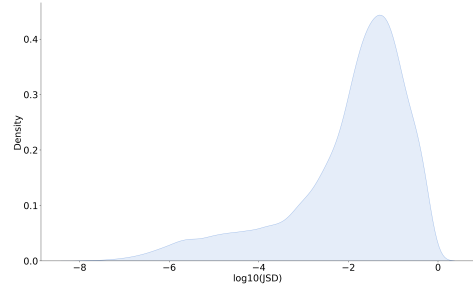


Figure 6: 500 random images from the MSCOCO dataset captioned by LLaVA-1.5. For each next-token prediction, we statistic the JS divergence (JSD) between two logit distributions produced by different images.

essential priors should remain highly consistent across diverse visual inputs. This intrinsic property provides a reliable basis for distinguishing between essential and detrimental priors.

We employ the Jensen-Shannon (JS) divergence to measure the consistency between two logit distributions produced from different images:

$$\mathcal{D}_{JS} = JS(p_{\theta}(y_t | v, x, y_{<t}) || p_{\theta}(y_t | v', x, y_{<t})) \quad (5)$$

where $p_{\theta}(y_t | v, x, y_{<t})$ is defined in Eq.1. The statistical results are visualized in Fig.6. We observe that the JSD values can be clearly separated into two distinct ranges: $\log_{10}(\mathcal{D}_{JS}) > -4$ and $\log_{10}(\mathcal{D}_{JS}) \leq -4$. Higher JSD values are associated with detrimental priors, while lower values correspond to essential priors, as shown in Fig.3 and Fig.4. Based on this observation, we set a threshold of $\gamma = -4$ to distinguish between the two types of priors. Further discussion can be found in Appendix. C.3

Setting	Method	LLaVA-1.5		InstructBLIP		Qwen-VL-Chat	
		Acc. \uparrow	F1 \uparrow	Acc. \uparrow	F1 \uparrow	Acc. \uparrow	F1 \uparrow
Random	Regular	83.47	82.25	80.49	81.10	82.32	79.35
	VCD	85.30	84.59	81.75	82.06	<u>84.74</u>	<u>82.80</u>
	ICD	84.81	83.44	80.95	81.59	83.10	80.52
	IBD	85.36	84.28	74.82	77.87	83.07	80.23
	DeFG	<u>86.68</u>	<u>85.71</u>	84.35	<u>84.50</u>	84.04	81.49
	CICD	87.85	87.77	<u>84.00</u>	84.89	87.54	86.37
Popular	Regular	79.56	78.99	76.59	78.16	81.11	78.34
	VCD	80.81	80.84	77.22	78.60	82.95	<u>81.17</u>
	ICD	81.44	80.53	76.82	78.48	81.26	78.87
	IBD	81.68	81.13	69.35	74.31	82.20	79.59
	DeFG	<u>82.96</u>	<u>82.46</u>	<u>79.25</u>	<u>80.46</u>	<u>83.02</u>	80.57
	CICD	84.83	85.18	81.01	82.53	85.94	84.90
Adversarial	Regular	76.95	77.13	72.89	75.58	78.23	75.72
	VCD	77.27	78.19	74.03	76.39	80.37	<u>78.96</u>
	ICD	78.07	77.98	73.19	75.91	79.03	77.05
	IBD	78.26	78.52	66.60	72.63	79.68	77.36
	DeFG	79.40	<u>79.69</u>	<u>75.19</u>	<u>77.52</u>	<u>80.42</u>	78.24
	CICD	<u>78.60</u>	80.30	75.55	78.63	81.94	81.37

Table 1: Results on POPE. **Acc.** and **F1** represent the average accuracy and F1-score across three datasets (MSCOCO, A-OKVQA, and GQA), respectively. The **bolded** results denote the best in each setting, and the underlined results denote the second-best.

4.3 Cross-Images Contrastive Decoding

After completing the above preparation, we integrate the proposed method into the contrastive decoding process. Specifically, the model performs regular decoding when essential priors are detected and applies contrastive decoding to suppress detrimental priors. In the case of detrimental priors, smaller distributional differences imply a stronger detrimental effect. Accordingly, we define the contrastive coefficient α in Eq. 3 as: $\alpha = 1 - \log_{10}(\mathcal{D}_{JS})$. Based on the observed density of \mathcal{D}_{JS} values, we clip α to the interval $[1, 3]$ to ensure numerical stability.

The final logit distribution is defined as follows:

$$\text{logit}_{CICD}(y_t | v, x, y_{<t}) = \begin{cases} \text{logit}_{\theta}(y_t | v, x, y_{<t}) & \text{if } \mathcal{D}_{JS} \leq \gamma \\ \text{logit}_{CD}(y_t | v, x, y_{<t}) & \text{if } \mathcal{D}_{JS} > \gamma \end{cases} \quad (6)$$

where $\text{logit}_{\theta}(y_t | v, x, y_{<t})$ is defined in Eq. 1, and $\text{logit}_{CD}(y_t | v, x, y_{<t})$ is defined in Eq. 3.

5 Experiment

5.1 Experiment Settings

Due to space constraints, we present only the key aspects of our experimental setup here. Detailed settings can be found in Sec.B.

Benchmarks We evaluate the performance of CICD across 4 widely adopted multimodal hallucination benchmarks to validate its effectiveness on different tasks. These include two generative benchmarks (CHAIR (Rohrbach et al., 2018) and DetailCaps (Ye et al., 2025)), one discriminative benchmark (POPE (Li et al., 2023b)), and one hybrid benchmark (AMBER (Wang et al., 2024a)).

Evaluated LVLMS We evaluate the generalizability of CICD across 6 LVLMS from three model families: InstructBLIP (Dai et al., 2023), the LLaVA series (LLaVA-1.5 (Liu et al., 2024c) and LLaVA-Next (Liu et al., 2024d)), and the Qwen series (Qwen-VL-Chat (Bai et al., 2023b), Qwen2-VL-Instruct (Wang et al., 2024b), and Qwen2.5-VL-Instruct (Bai et al., 2025)). Unless stated otherwise, all models are implemented at the 7B scale.

Baselines We compare CICD with 4 recent training-free methods that specifically target language priors: VCD (Leng et al., 2024), ICD (Wang et al., 2024c), IBD (Zhu et al., 2024b), and DeFG (Zhang et al., 2025). All of these methods construct negative contexts based on the original image. In contrast, we identify several limitations of this approach and propose CICD as a more effective alternative.

MaxLen	Method	LLaVA-1.5				InstructBLIP			
		Cs↓	Ci↓	Recall	Length	Cs↓	Ci↓	Recall	Length
64	Regular	24.4	8.9	56.6	53.7	35.6	13.2	56.4	54.8
	VCD	25.0	8.3	59	54.0	32.2	10.3	60.6	55.2
	ICD	23.2	8.1	58.4	54.4	29.8	9.8	60.6	55.7
	IBD	<u>21.2</u>	<u>6.9</u>	58.8	54.5	<u>27.8</u>	<u>9.2</u>	60.3	56.1
	DeFG	22.4	7.2	58.2	54.4	32.4	11	59.4	56.0
	CICD	18.0	6.1	59.6	53.3	23.8	7.7	62.2	54.8
512	Regular	<u>54.6</u>	16.4	72.6	106.8	62.6	19.5	66.9	113.6
	VCD	59.8	17.8	75.6	104	64.8	18.8	71.9	108.6
	ICD	57.0	<u>15.0</u>	74.6	103.3	59.0	17.1	69.2	108.5
	IBD	57.6	16.5	74.2	104.3	<u>57.6</u>	<u>15.7</u>	70.8	118.5
	DeFG	57.4	16.3	75.5	102.8	59.0	17.7	71.5	108.9
	CICD	43.8	11.7	75.0	103.3	49.8	13.7	70.3	98.8

Table 2: Results on the test set of CHAIR. *MaxLen* denotes the maximum generation length. *Cs* and *Ci* represent *CHAIRs* and *CHAIRi* respectively.

Model	Method	Generative				Discriminative				
		CHAIR↓	Cover↑	Hal↓	Cog↓	Acc.↑	Prec.↑	Recall↑	F1↑	AMBER↑
LLaVA-1.5	Regular	11.6	49.7	47.7	4.4	67.4	83.9	61.8	71.2	79.80
	VCD	9.8	<u>51.2</u>	43.8	4.4	68.1	85.1	61.0	71.1	80.65
	ICD	8.8	<u>51.2</u>	<u>38.7</u>	<u>4.1</u>	<u>70.3</u>	86.0	64.1	73.4	<u>82.30</u>
	IBD	9.8	50.5	42.2	4.4	69.2	86.3	62.1	72.2	81.20
	DeFG	9.1	50.7	39.9	<u>4.1</u>	70.2	<u>86.8</u>	<u>63.0</u>	73.0	81.95
	CICD	6.6	52.7	34.8	2.2	71.1	89.4	61.9	<u>73.1</u>	83.25
InstructBLIP	Regular	12.4	51.9	52.4	5.0	68.3	78.6	71.7	75	81.30
	VCD	9.9	54.0	44.6	<u>4.2</u>	70.6	80.6	<u>72.7</u>	76.4	83.25
	ICD	9.8	53.9	46.7	5.1	69.9	80.3	<u>70.9</u>	75.3	82.75
	IBD	<u>9.0</u>	56.1	45.1	4.6	54.2	86.3	34.2	49.0	70.00
	DeFG	9.7	<u>54.1</u>	<u>44.5</u>	5.2	<u>72.1</u>	80.7	75.1	77.8	<u>84.05</u>
	CICD	7.1	53.6	35.0	2.3	72.8	<u>85.4</u>	70.1	<u>77.0</u>	84.95

Table 3: Results on AMBER. The maximum generation length is 512. *AMBER* metric is calculated by $(100 - CHAIR + F1)/2$.

5.2 Implementation Details

We use sampling decoding for next-token prediction with default settings. Following (Leng et al., 2024), we incorporate adaptive plausibility constraints into the decoding process. We use the MSCOCO 2014 validation set as the image retrieval corpus, which contains 40,504 images. All experiments are conducted on an NVIDIA RTX 3090 GPU.

5.3 Main Results

Results on POPE As shown in Tab. 1, our method achieves the highest F1 scores across all experimental settings. This suggests that we can utilize cross-image consistency to effectively alleviate language priors and promote LVLMS to convey faithful visual information. The *Popular* setting uses frequent objects for negative samples, increas-

ing susceptibility to language priors. The strong performance gains of our method in this setting highlight its effectiveness in mitigating such priors.

Results on CHAIR The results in Tab. 2 demonstrate our method’s superior performance across all experimental conditions, with particularly pronounced improvements observed at longer generation lengths. Longer context lengths amplify the model’s susceptibility to language priors, making these experimental results particularly compelling evidence of our method’s efficacy in mitigating such priors. Compared to baselines, our method’s principal advantage lies in its complete preservation of visual information and essential language priors, which is directly reflected in the superior performance in image captioning.

Method	LLaVA-1.5			InstructBLIP			Qwen-VL-Chat		
	Cs↓	Ci↓	CAP↑	Cs↓	Ci↓	CAP↑	Cs↓	Ci↓	CAP↑
Regular	55.7	17.4	52.60	58.6	18.0	52.99	9.9	7.3	30.73
VCD	55.7	16.8	<u>52.91</u>	59.6	18.9	53.20	7.3	5.9	<u>31.28</u>
ICD	<u>53.9</u>	<u>16.6</u>	52.82	<u>55.7</u>	16.7	53.24	<u>5.6</u>	7.0	29.70
IBD	54.1	15.8	52.48	56.4	<u>15.5</u>	<u>54.14</u>	4.6	2.9	29.31
DeFG	55.7	<u>16.6</u>	52.72	59.1	17.4	53.06	5.6	3.9	30.21
CICD	45.6	13.1	55.80	45.7	13.2	54.20	5.9	<u>3.5</u>	31.34

Table 4: Results on the COCO subset of DetailCaps. The maximum generation length is 512. *Cs*, *Ci*, and *CAP* represent *CHAIRs*, *CHAIRi*, and *CAPTURE* respectively.

Model	Method	CHAIR(MaxLen=512)			POPE (F1↑)		
		Cs↓	Ci↓	Recall	Random	Popular	Adversarial
LLaVA-Next	Regular	41.8	11.9	60.2	85.47	83.14	79.87
	CICD	37.6	10.4	62.7	88.22	86.29	82.76
Qwen2-VL-Instruct	Regular	53.8	10.0	69.4	88.33	85.82	82.43
	CICD	50.6	9.4	73.6	90.67	88.07	84.53
Qwen2.5-VL-Instruct	Regular	41.2	11.5	65.7	87.83	85.66	83.12
	CICD	39.4	9.6	68.1	89.95	88.00	84.75

Table 5: Results on more LVLMS. *F1* is the average F1-score across three datasets (MSCOCO, A-OKVQA, and GQA).

Results on AMBER As illustrated in Tab. 3, our method achieves the lowest hallucination frequency in generative tasks while simultaneously attaining state-of-the-art performance on the comprehensive AMBER metric. Language prior is particularly critical for generative tasks, where language priors manifest more severely than in discriminative tasks, explaining our method’s pronounced advantages in image captioning.

Results on DetailCaps Tab. 4 presents the evaluation results on DetailCaps. The *CAPTURE* metric quantitatively evaluates caption quality through both lexical matching and semantic alignment, measuring the consistency of key content (entities, attributes, and relations) between generated captions and multiple ground-truth references. Our method achieves the best performance across all three evaluated LVLMS, demonstrating its robust capability to mitigate language priors and significantly enhance image captioning performance.

5.4 Effectiveness on More LVLMS

To comprehensively demonstrate the effectiveness and generalizability of our method, we select three of the most recent open-source LVLMS to conduct experiments. The results are presented in Tab. 5. Our method demonstrates significant performance improvements in all experiments, consistently re-

ducing hallucinations across both generative and discriminative tasks through effective mitigation of language priors. We also test our method on these LVLMS by *DetailCaps* and the results are shown in Tab. 6. The improvements observed across different LVLMS confirm our method’s practical advantages: an elegantly simple framework coupled with state-of-the-art effectiveness.

Further experiments will be discussed in Sec. B.

6 Conclusion

In this paper, we mitigate the influence of language priors in LVLMS. Through a comprehensive investigation, we reveal that language priors are intrinsic to the model and remain consistent across different images. Building on this observation, we propose Cross-Image Contrastive Decoding (CICD) — a training-free method that effectively mitigates language priors while preserving visual information. Extensive experiments across multiple benchmarks and LVM architectures demonstrate the effectiveness of CICD, particularly in image captioning tasks where language priors are most prominent.

The simplicity and efficiency of CICD offer strong practical potential, enabling seamless integration with other hallucination mitigation methods to further enhance LVM performance. This integration forms a key direction for our future work.

7 Limitation

We observe that language priors remain consistent across different images. Based on this insight, we propose the Cross-Images Contrastive Decoding (CICD) method to eliminate language priors. Our method has two main limitations compared to regular decoding. First, it requires an additional image that differs sufficiently from the original input. Second, both the original and the additional images must undergo separate forward passes to obtain their respective logit distributions for contrastive decoding.

Additional Image While the additional image is necessary, there is no strict requirement on its degree of difference from the original. Hallucinations typically occur in content-rich elements such as objects, attributes, and relationships, which naturally exhibit substantial variability across real-world images. Furthermore, our experiments demonstrate that the effectiveness of hallucination mitigation is not strongly correlated with image similarity. The experimental results demonstrate that randomly selected images perform comparably to retrieved ones, highlighting the practical applicability of our method. This flexibility significantly lowers the barrier for real-world deployment.

Twice Forward Propagation Although performing twice forward propagations doubles the theoretical computational cost, in practice, we merge the two inputs into a single batch and perform one forward propagation with a doubled batch size to achieve the same effect. Under this implementation, our method incurs only a 10% increase in inference time and a 5% increase in memory usage, demonstrating strong potential for practical deployment.

References

- Jinze Bai, Shuai Bai, Yunfei Chu, Zeyu Cui, Kai Dang, Xiaodong Deng, Yang Fan, Wenbin Ge, Yu Han, Fei Huang, and 1 others. 2023a. *Qwen technical report*. *arXiv preprint arXiv:2309.16609*.
- Jinze Bai, Shuai Bai, Shusheng Yang, Shijie Wang, Sinan Tan, Peng Wang, Junyang Lin, Chang Zhou, and Jingren Zhou. 2023b. *Qwen-vl: A versatile vision-language model for understanding, localization, text reading, and beyond*. *Preprint*, arXiv:2308.12966.
- Shuai Bai, Keqin Chen, Xuejing Liu, Jialin Wang, Wenbin Ge, Sibao Song, Kai Dang, Peng Wang, Shijie Wang, Jun Tang, Humen Zhong, Yuezhi Zhu, Mingkun Yang, Zhaohai Li, Jianqiang Wan, Pengfei Wang, Wei Ding, Zheren Fu, Yiheng Xu, and 8 others. 2025. *Qwen2.5-vl technical report*. *Preprint*, arXiv:2502.13923.
- Tom B. Brown, Benjamin Mann, Nick Ryder, Melanie Subbiah, Jared Kaplan, Prafulla Dhariwal, Arvind Neelakantan, Pranav Shyam, Girish Sastry, Amanda Askell, Sandhini Agarwal, Ariel Herbert-Voss, Gretchen Krueger, Tom Henighan, Rewon Child, Aditya Ramesh, Daniel M. Ziegler, Jeffrey Wu, Clemens Winter, and 12 others. 2020. *Language models are few-shot learners*. *Preprint*, arXiv:2005.14165.
- Cong Chen, Mingyu Liu, Chenchen Jing, Yizhou Zhou, Fengyun Rao, Hao Chen, Bo Zhang, and Chunhua Shen. 2025. *PerturboLLaVA: Reducing multimodal hallucinations with perturbative visual training*. In *The Thirteenth International Conference on Learning Representations*.
- Wei-Lin Chiang, Zhuohan Li, Ziqing Lin, Ying Sheng, Zhanghao Wu, Hao Zhang, Lianmin Zheng, Siyuan Zhuang, Yonghao Zhuang, Joseph E Gonzalez, and 1 others. 2023. Vicuna: An open-source chatbot impressing gpt-4 with 90%* chatgpt quality. *See https://vicuna.lmsys.org (accessed 14 April 2023)*, 2(3):6.
- Yung-Sung Chuang, Yujia Xie, Hongyin Luo, Yoon Kim, James R. Glass, and Pengcheng He. 2024. *Dola: Decoding by contrasting layers improves factuality in large language models*. In *The Twelfth International Conference on Learning Representations, ICLR 2024, Vienna, Austria, May 7-11, 2024*. OpenReview.net.
- Wenliang Dai, Junnan Li, Dongxu Li, Anthony Meng Huat Tiong, Junqi Zhao, Weisheng Wang, Boyang Li, Pascale Fung, and Steven C. H. Hoi. 2023. *Instructblip: Towards general-purpose vision-language models with instruction tuning*. In *Advances in Neural Information Processing Systems 36: Annual Conference on Neural Information Processing Systems 2023, NeurIPS 2023, New Orleans, LA, USA, December 10 - 16, 2023*.
- Alexey Dosovitskiy, Lucas Beyer, Alexander Kolesnikov, Dirk Weissenborn, Xiaohua Zhai, Thomas Unterthiner, Mostafa Dehghani, Matthias Minderer, Georg Heigold, Sylvain Gelly, Jakob Uszkoreit, and Neil Houlsby. 2021. *An image is worth 16x16 words: Transformers for image recognition at scale*. In *9th International Conference on Learning Representations, ICLR 2021, Virtual Event, Austria, May 3-7, 2021*. OpenReview.net.
- Anisha Gunjal, Jihan Yin, and Erhan Bas. 2024. *Detecting and preventing hallucinations in large vision language models*. In *Thirty-Eighth AAAI Conference on Artificial Intelligence, AAAI 2024, Thirty-Sixth Conference on Innovative Applications of Artificial Intelligence, IAAI 2024, Fourteenth Symposium on Educational Advances in Artificial Intelligence, EAAI*

- 2014, February 20-27, 2024, Vancouver, Canada, pages 18135–18143. AAAI Press.
- Qidong Huang, Xiaoyi Dong, Pan Zhang, Bin Wang, Conghui He, Jiaqi Wang, Dahua Lin, Weiming Zhang, and Nenghai Yu. 2024. [OPERA: alleviating hallucination in multi-modal large language models via over-trust penalty and retrospection-allocation](#). In *IEEE/CVF Conference on Computer Vision and Pattern Recognition, CVPR 2024, Seattle, WA, USA, June 16-22, 2024*, pages 13418–13427. IEEE.
- Ziwei Ji, Nayeon Lee, Rita Frieske, Tiezheng Yu, Dan Su, Yan Xu, Etsuko Ishii, Yejin Bang, Andrea Madotto, and Pascale Fung. 2023. [Survey of hallucination in natural language generation](#). *ACM Comput. Surv.*, 55(12):248:1–248:38.
- Liqiang Jing, Ruosen Li, Yunmo Chen, and Xinya Du. 2024. [Faithscore: Fine-grained evaluations of hallucinations in large vision-language models](#). In *Findings of the Association for Computational Linguistics: EMNLP 2024, Miami, Florida, USA, November 12-16, 2024*, pages 5042–5063. Association for Computational Linguistics.
- Seil Kang, Jinyeong Kim, Junhyeok Kim, and Seong Jae Hwang. 2025. [See what you are told: Visual attention sink in large multimodal models](#). *CoRR*, abs/2503.03321.
- Sicong Leng, Hang Zhang, Guanzheng Chen, Xin Li, Shijian Lu, Chunyan Miao, and Lidong Bing. 2024. [Mitigating object hallucinations in large vision-language models through visual contrastive decoding](#). In *IEEE/CVF Conference on Computer Vision and Pattern Recognition, CVPR 2024, Seattle, WA, USA, June 16-22, 2024*, pages 13872–13882. IEEE.
- Jiaming Li, Jiacheng Zhang, Zequn Jie, Lin Ma, and Guanbin Li. 2025. [Mitigating hallucination for large vision language model by inter-modality correlation calibration decoding](#). *CoRR*, abs/2501.01926.
- Xiang Lisa Li, Ari Holtzman, Daniel Fried, Percy Liang, Jason Eisner, Tatsunori Hashimoto, Luke Zettlemoyer, and Mike Lewis. 2023a. [Contrastive decoding: Open-ended text generation as optimization](#). In *Proceedings of the 61st Annual Meeting of the Association for Computational Linguistics (Volume 1: Long Papers)*, pages 12286–12312, Toronto, Canada. Association for Computational Linguistics.
- Yifan Li, Yifan Du, Kun Zhou, Jinpeng Wang, Wayne Xin Zhao, and Ji-Rong Wen. 2023b. [Evaluating object hallucination in large vision-language models](#). In *Proceedings of the 2023 Conference on Empirical Methods in Natural Language Processing, EMNLP 2023, Singapore, December 6-10, 2023*, pages 292–305. Association for Computational Linguistics.
- Yifan Li, Yifan Du, Kun Zhou, Jinpeng Wang, Wayne Xin Zhao, and Ji-Rong Wen. 2023c. [Evaluating object hallucination in large vision-language models](#). In *Proceedings of the 2023 Conference on Empirical Methods in Natural Language Processing, EMNLP 2023, Singapore, December 6-10, 2023*, pages 292–305. Association for Computational Linguistics.
- Tsung-Yi Lin, Michael Maire, Serge J. Belongie, James Hays, Pietro Perona, Deva Ramanan, Piotr Dollár, and C. Lawrence Zitnick. 2014. [Microsoft COCO: common objects in context](#). In *Computer Vision - ECCV 2014 - 13th European Conference, Zurich, Switzerland, September 6-12, 2014, Proceedings, Part V*, volume 8693 of *Lecture Notes in Computer Science*, pages 740–755. Springer.
- Fuxiao Liu, Kevin Lin, Linjie Li, Jianfeng Wang, Yaser Yacoob, and Lijuan Wang. 2024a. [Mitigating hallucination in large multi-modal models via robust instruction tuning](#). In *The Twelfth International Conference on Learning Representations, ICLR 2024, Vienna, Austria, May 7-11, 2024*. OpenReview.net.
- Hanchao Liu, Wenyuan Xue, Yifei Chen, Dapeng Chen, Xiutian Zhao, Ke Wang, Liping Hou, Rongjun Li, and Wei Peng. 2024b. [A survey on hallucination in large vision-language models](#). *CoRR*, abs/2402.00253.
- Haotian Liu, Chunyuan Li, Yuheng Li, and Yong Jae Lee. 2024c. Improved baselines with visual instruction tuning. In *Proceedings of the IEEE/CVF Conference on Computer Vision and Pattern Recognition (CVPR)*, pages 26296–26306.
- Haotian Liu, Chunyuan Li, Yuheng Li, Bo Li, Yuanhan Zhang, Sheng Shen, and Yong Jae Lee. 2024d. [Llava-next: Improved reasoning, ocr, and world knowledge](#).
- Haotian Liu, Chunyuan Li, Qingyang Wu, and Yong Jae Lee. 2023. [Visual instruction tuning](#). In *Advances in Neural Information Processing Systems 36: Annual Conference on Neural Information Processing Systems 2023, NeurIPS 2023, New Orleans, LA, USA, December 10 - 16, 2023*.
- Holy Lovenia, Wenliang Dai, Samuel Cahyawijaya, Ziwei Ji, and Pascale Fung. 2024. [Negative object presence evaluation \(NOPE\) to measure object hallucination in vision-language models](#). In *Proceedings of the 3rd Workshop on Advances in Language and Vision Research (ALVR)*, pages 37–58, Bangkok, Thailand. Association for Computational Linguistics.
- Jiaying Lu, Jinneng Rao, Kezhen Chen, Xiaoyuan Guo, Yawen Zhang, Baochen Sun, Carl Yang, and Jie Yang. 2024. [Evaluation and enhancement of semantic grounding in large vision-language models](#). *Preprint*, arXiv:2309.04041.
- OpenAI, :, Aaron Hurst, Adam Lerer, Adam P. Goucher, Adam Perelman, Aditya Ramesh, Aidan Clark, AJ Ostrow, Akila Welihinda, Alan Hayes, Alec Radford, Aleksander Mądry, Alex Baker-Whitcomb, Alex Beutel, Alex Borzunov, Alex Carney, Alex Chow, Alex Kirillov, and 401 others. 2024. [Gpt-4o system card](#). *Preprint*, arXiv:2410.21276.

- Alec Radford, Jong Wook Kim, Chris Hallacy, Aditya Ramesh, Gabriel Goh, Sandhini Agarwal, Girish Sastry, Amanda Askell, Pamela Mishkin, Jack Clark, Gretchen Krueger, and Ilya Sutskever. 2021. [Learning transferable visual models from natural language supervision](#). In *Proceedings of the 38th International Conference on Machine Learning, ICML 2021, 18-24 July 2021, Virtual Event*, volume 139 of *Proceedings of Machine Learning Research*, pages 8748–8763. PMLR.
- Hanoona Rasheed, Muhammad Maaz, Sahal Shaji, Abdelrahman Shaker, Salman Khan, Hisham Cholakkal, Rao M Anwer, Eric Xing, Ming-Hsuan Yang, and Fahad S Khan. 2024. Glamm: Pixel grounding large multimodal model. In *Proceedings of the IEEE/CVF Conference on Computer Vision and Pattern Recognition*, pages 13009–13018.
- Anna Rohrbach, Lisa Anne Hendricks, Kaylee Burns, Trevor Darrell, and Kate Saenko. 2018. [Object hallucination in image captioning](#). In *Proceedings of the 2018 Conference on Empirical Methods in Natural Language Processing*, pages 4035–4045, Brussels, Belgium. Association for Computational Linguistics.
- Gemini Team, Petko Georgiev, Ving Ian Lei, Ryan Burnell, Libin Bai, Anmol Gulati, Garrett Tanzer, Damien Vincent, Zhufeng Pan, Shibo Wang, Soroosh Mariooryad, Yifan Ding, Xinyang Geng, Fred Alcober, Roy Frostig, Mark Omernick, Lexi Walker, Cosmin Paduraru, Christina Sorokin, and 1118 others. 2024. [Gemini 1.5: Unlocking multimodal understanding across millions of tokens of context](#). *Preprint*, arXiv:2403.05530.
- Hugo Touvron, Thibaut Lavril, Gautier Izacard, Xavier Martinet, Marie-Anne Lachaux, Timothée Lacroix, Baptiste Rozière, Naman Goyal, Eric Hambro, Faisal Azhar, and 1 others. 2023. Llama: Open and efficient foundation language models. *arXiv preprint arXiv:2302.13971*.
- Laurens van der Maaten and Geoffrey Hinton. 2008. [Visualizing data using t-sne](#). *Journal of Machine Learning Research*, 9(86):2579–2605.
- Junyang Wang, Yuhang Wang, Guohai Xu, Jing Zhang, Yukai Gu, Haitao Jia, Jiaqi Wang, Haiyang Xu, Ming Yan, Ji Zhang, and Jitao Sang. 2024a. [Amber: An llm-free multi-dimensional benchmark for mllms hallucination evaluation](#). *Preprint*, arXiv:2311.07397.
- Junyang Wang, Yiyang Zhou, Guohai Xu, Pengcheng Shi, Chenlin Zhao, Haiyang Xu, Qinghao Ye, Ming Yan, Ji Zhang, Jihua Zhu, Jitao Sang, and Haoyu Tang. 2023. [Evaluation and analysis of hallucination in large vision-language models](#). *CoRR*, abs/2308.15126.
- Peng Wang, Shuai Bai, Sinan Tan, Shijie Wang, Zhihao Fan, Jinze Bai, Keqin Chen, Xuejing Liu, Jialin Wang, Wenbin Ge, Yang Fan, Kai Dang, Mengfei Du, Xuancheng Ren, Rui Men, Dayiheng Liu, Chang Zhou, Jingren Zhou, and Junyang Lin. 2024b. [Qwen2-vl: Enhancing vision-language model’s perception of the world at any resolution](#). *Preprint*, arXiv:2409.12191.
- Xintong Wang, Jingheng Pan, Liang Ding, and Chris Biemann. 2024c. [Mitigating hallucinations in large vision-language models with instruction contrastive decoding](#). In *Findings of the Association for Computational Linguistics, ACL 2024, Bangkok, Thailand and virtual meeting, August 11-16, 2024*, pages 15840–15853. Association for Computational Linguistics.
- Jason Wei, Xuezhi Wang, Dale Schuurmans, Maarten Bosma, Fei Xia, Ed Chi, Quoc V Le, Denny Zhou, and 1 others. 2022. Chain-of-thought prompting elicits reasoning in large language models. *Advances in neural information processing systems*, 35:24824–24837.
- Yike Wu, Yu Zhao, Shiwan Zhao, Ying Zhang, Xiaojie Yuan, Guoqing Zhao, and Ning Jiang. 2022. [Overcoming language priors in visual question answering via distinguishing superficially similar instances](#). In *Proceedings of the 29th International Conference on Computational Linguistics*, pages 5721–5729, Gyeongju, Republic of Korea. International Committee on Computational Linguistics.
- Zhengyuan Yang, Linjie Li, Kevin Lin, Jianfeng Wang, Chung-Ching Lin, Zicheng Liu, and Lijuan Wang. 2023. [The dawn of lmms: Preliminary explorations with gpt-4v\(ision\)](#). *Preprint*, arXiv:2309.17421.
- Qinghao Ye, Xianhan Zeng, Fu Li, Chunyuan Li, and Haoqi Fan. 2025. [Painting with words: Elevating detailed image captioning with benchmark and alignment learning](#). In *The Thirteenth International Conference on Learning Representations*.
- Hao Yin, Guangzong Si, and Zilei Wang. 2025. [Clear-sight: Visual signal enhancement for object hallucination mitigation in multimodal large language models](#). *CoRR*, abs/2503.13107.
- Haoxuan You, Haotian Zhang, Zhe Gan, Xianzhi Du, Bowen Zhang, Zirui Wang, Liangliang Cao, Shih-Fu Chang, and Yinfei Yang. 2024. [Ferret: Refer and ground anything anywhere at any granularity](#). In *The Twelfth International Conference on Learning Representations*.
- Weihao Yu, Zhengyuan Yang, Linjie Li, Jianfeng Wang, Kevin Lin, Zicheng Liu, Xinchao Wang, and Lijuan Wang. 2024. [MM-vet: Evaluating large multimodal models for integrated capabilities](#). In *Proceedings of the 41st International Conference on Machine Learning*, volume 235 of *Proceedings of Machine Learning Research*, pages 57730–57754. PMLR.
- Ce Zhang, Zifu Wan, Zhehan Kan, Martin Q. Ma, Simon Stepputtis, Deva Ramanan, Russ Salakhutdinov, Louis-Philippe Morency, Katia P. Sycara, and Yaqi Xie. 2025. [Self-correcting decoding with generative feedback for mitigating hallucinations in large vision-language models](#). In *The Thirteenth International Conference on Learning Representations*.

Ren Zhibo, Wang Huizhen, Zhu Muhua, Wang Yichao, Xiao Tong, and Zhu Jingbo. 2023. [Overcoming language priors with counterfactual inference for visual question answering](#). In *Proceedings of the 22nd Chinese National Conference on Computational Linguistics*, pages 600–610, Harbin, China. Chinese Information Processing Society of China.

Deyao Zhu, Jun Chen, Xiaoqian Shen, Xiang Li, and Mohamed Elhoseiny. 2024a. [Minigpt-4: Enhancing vision-language understanding with advanced large language models](#). In *The Twelfth International Conference on Learning Representations, ICLR 2024, Vienna, Austria, May 7-11, 2024*. OpenReview.net.

Lanyun Zhu, Deyi Ji, Tianrun Chen, Peng Xu, Jieping Ye, and Jun Liu. 2024b. [IBD: alleviating hallucinations in large vision-language models via image-biased decoding](#). *CoRR*, abs/2402.18476.

Younan Zhu, Linwei Tao, Minjing Dong, and Chang Xu. 2025. [Mitigating object hallucinations in large vision-language models via attention calibration](#). *CoRR*, abs/2502.01969.

A Detailed Related Work

A.1 Large Vision-Language Models

Typically, Large Vision-Language Models (LVLMs) (Dai et al., 2023; Liu et al., 2024c; Bai et al., 2023b; Zhu et al., 2024a) consist of a visual encoder (Radford et al., 2021; Dosovitskiy et al., 2021) and a Large Language Model (LLM) backbone (Touvron et al., 2023; Chiang et al., 2023). The visual encoder extracts visual features, which are then aligned with text tokens through a fusion module to form the input context for the LLM. Through multi-stage training, including modality alignment and instruction tuning (Liu et al., 2023), LVLMs acquire the ability to perform various multimodal tasks such as image captioning (Ye et al., 2025), visual question answering (Yu et al., 2024), and visual grounding (Lu et al., 2024). Despite significant advancements, LVLMs still suffer from severe hallucination problems, often generating content that contradicts the visual input.

A.2 Hallucination in LVLMs

Originally, hallucinations (Ji et al., 2023; Liu et al., 2024b) were defined as undesirable outputs or non-factual information. In the multimodal domain, the study of hallucinations primarily focuses on cross-modal consistency (Li et al., 2023c; Wang et al., 2023), requiring that LVLM-generated content remains faithful to the visual inputs. Multiple factors contribute to hallucinations in LVLMs, including biased visual attention (Zhu et al., 2025; Li et al., 2025), attention misallocation (Huang et al., 2024; Yin et al., 2025; Kang et al., 2025), and language priors (Leng et al., 2024; Zhu et al., 2024b; Wang et al., 2024c). Among these, language priors are the most direct cause, making it difficult for LVLMs to accurately express their understanding of visual information.

A.3 Language Priors

As LVLMs are built upon LLMs, they inherently inherit the linguistic knowledge embedded in LLMs, which are referred to as language priors (Zhibo et al., 2023; Wu et al., 2022). Language priors specifically manifest when LVLMs generate content that is linguistically plausible but inconsistent with visual evidence. Some works (Chen et al., 2025; Liu et al., 2024a; Gunjal et al., 2024) meticulously design specialized training data to mitigate this issue. However, such training-based approaches exhibit limited generalizability and can-

not be easily transferred to broader application scenarios. Recently, a series of training-free approaches have directly reduced language priors using contrastive decoding (Li et al., 2023a; Chuang et al., 2024), achieving remarkable performance. These methods construct an alternative logit distribution on top of the original one through techniques such as masking the image (Leng et al., 2024), perturbing the instruction (Wang et al., 2024c), augmenting the vision input (Zhu et al., 2024b), or performing cross-modal conversion (Zhang et al., 2025). During decoding, the two logit distributions are contrasted to eliminate language priors.

While these methods effectively mitigate linguistic priors, they inevitably incur visual information loss during contrastive decoding due to information overlap, where both distributions share partial visual features. Through a comprehensive analysis of language priors, we identify their vision-independent nature. Based on this insight, we propose the Cross-Images Contrastive Decoding (CICD) method, which eliminates language priors by leveraging their consistency across different images, while preserving visual information through inter-image variation.

B Detailed Experiment Settings

B.1 Benchmarks

In order to validate the effectiveness of our method in mitigating language hallucination, we evaluate its performance on four widely-used multimodal hallucination benchmarks: two generative benchmarks (CHAIR (Rohrbach et al., 2018) and Detail-Caps (Ye et al., 2025)), one discriminative benchmark (POPE (Li et al., 2023b)), and one hybrid benchmark (AMBER (Wang et al., 2024a)).

CHAIR evaluates the proportion of hallucinated objects, which are generated by the model but not present in the reference annotations. Following prior works, we randomly select 500 images from the MSCOCO (Lin et al., 2014) dataset as the test set. We additionally select another 500 images to construct a validation set for hyperparameter tuning. This benchmark includes two metrics: CHAIRs and CHAIRi, defined as follows:

$$\begin{aligned}\text{CHAIRs} &= \frac{|\text{Hallucinated Objects}|}{|\text{All Objects}|}, \\ \text{CHAIRi} &= \frac{|\text{Hallucinated Sentences}|}{|\text{All Sentences}|}\end{aligned}\tag{7}$$

Method	LLaVA-Next			Qwen2-VL-Instruct			Qwen2.5-VL-Instruct		
	Cs↓	Ci↓	CAP↑	Cs↓	Ci↓	CAP↑	Cs↓	Ci↓	CAP↑
Regular	61.06	38.0	10.4	60.04	51.3	10.6	62.62	42.2	11.7
CICD	62.19	36.2	8.5	61.79	48.4	9.9	65.07	43.8	10.9

Table 6: Results on the COCO subset of DetailCaps with more LVLMs.

DetailCaps is a fine-grained image captioning benchmark, accompanied by ground-truth detail captions generated by GPT-4V (Yang et al., 2023), Gemini-1.5-Pro (Team et al., 2024), and GPT-4o (OpenAI et al., 2024) for evaluation. It contains 4,870 images collected from multiple datasets, and we use a subset of 700 images from MSCOCO to conduct our experiments. This benchmark primarily adopts the CAPTURE metric to evaluate caption quality. CAPTURE evaluates the alignment between generated and reference captions by calculating F1 scores using both hard and soft matching across entities ($F1_{obj}$), attributes ($F1_{attr}$), and relations ($F1_{rel}$). The final score is computed through a weighted aggregation of these components:

$$CAPTURE = \frac{\alpha F1_{obj} + \beta F1_{attr} + \gamma F1_{rel}}{\alpha + \beta + \gamma} \quad (8)$$

where $\alpha = 5, \beta = 5, \gamma = 2$

POPE is a widely adopted benchmark for evaluating object hallucinations by prompting LVLMs to identify whether a specific object is present in the image. It comprises three distinct datasets: *MSCOCO*, *A-OKVQA*, and *GQA*. Each dataset uses three different negative sampling settings: *Random*, *Popular*, and *Adversarial*. In total, it includes 9,000 questions and 1,500 images. Accuracy and F1 score are used as the primary evaluation metrics.

AMBER combines generative and discriminative tasks, and is evaluated on a curated set of 1,004 images. In addition to image captioning, it includes 14,216 questions designed to assess hallucinations in object, attribute, and relation recognition. AMBER contains multiple metrics: *CHAIR*, *Cover*, *Hal*, *Cog*. It provides an annotated objects list $A_{obj} = obj_1^A, obj_2^A, \dots, obj_n^A$, and the generated objects are labeled as R'_{obj} . Each metric is calcu-

lated as follows:

$$\begin{aligned} CHAIR &= 1 - \frac{\text{len}(R'_{obj} \cap A_{obj})}{\text{len}(R'_{obj})}, \\ Cover &= \frac{\text{len}(R'_{obj} \cap A_{obj})}{\text{len}(A_{obj})}, \\ Hal &= \frac{\{CHAIR > 0\}}{\{All\ Caps\}}, \\ Cog &= \frac{\text{len}(R'_{obj} \cap H_{obj})}{\text{len}(R'_{obj})}, \end{aligned} \quad (9)$$

where H_{obj} denotes the set of hallucinated target objects generated by the LVLMs, and *All Caps* refers to all generated captions.

B.2 Evaluated LVLMs

To demonstrate the generalizability of the proposed CICD as a broadly applicable plug-and-play module, we evaluate its performance across six different LVLMs spanning three model families: InstructBLIP (Dai et al., 2023), LLaVA-1.5 (Liu et al., 2024c), LLaVA-Next (Liu et al., 2024d), Qwen-VL-Chat (Bai et al., 2023b), Qwen2-VL-Instruct (Wang et al., 2024b), and Qwen2.5-VL-Instruct (Bai et al., 2025). InstructBLIP and LLaVA-1.5 are both built upon Vicuna-7B (Chiang et al., 2023) as their language backbone, while LLaVA-Next is based on LLaMA3. The Qwen-VL series, including Qwen2-VL-Instruct and Qwen2.5-VL-Instruct, is developed using the QwenLM framework. As for vision encoders, InstructBLIP, LLaVA-1.5, LLaVA-Next, and Qwen-VL-Chat utilize the pretrained CLIP model (Radford et al., 2021), whereas Qwen2-VL-Instruct and Qwen2.5-VL-Instruct adopt a fine-tuned ViT (Dosovitskiy et al., 2021). All models are implemented at the 8B parameter scale.

B.3 Baselines

We compare our method with several training-free baselines that specifically target language priors.

VCD (Leng et al., 2024) introduces noise into the input image to suppress language priors, and

Model	Method	CHAIR(MaxLen=512)			POPE (F1↑)		
		Cs↓	Ci↓	Recall	Random	Popular	Adversarial
LLaVA-1.5-13B	Regular	58.8	17.0	73.4	82.94	81.46	78.49
	CICD	44.4	12.9	76.0	87.92	85.68	80.99
INstructBLIP-13B	Regular	65.6	21.0	62.7	81.31	77.20	74.69
	CICD	44.0	11.6	65.7	87.52	83.60	78.96

Table 7: Results on larger LVLMS. The maximum generation length is 512.

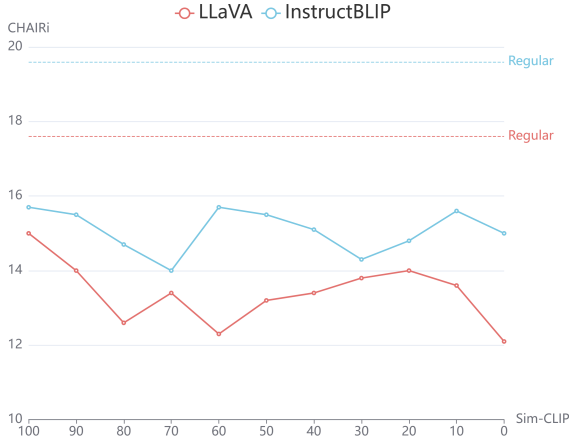


Figure 7: The correlation between similarity and performance. We conducted this experiment on the validation set of CHAIR. Sim-CLIP represents normalized image similarity, measured as the cosine distance between the features of two images extracted by CLIP.

then applies contrastive decoding for their elimination.

ICD (Wang et al., 2024c) constructs negative logits using adversarial instructions and enhances positive signals through contrastive decoding.

IBD (Zhu et al., 2024b) strengthens the model’s attention to visual features, thereby increasing the influence of image information during decoding.

DeFG (Zhang et al., 2025) converts the generated caption into an image and re-generates the caption from that image, leveraging the preserved visual content to reduce hallucinations.

C More Experiment Results

C.1 Effectiveness on Larger LVLMS

We evaluate the effectiveness of our method on larger models using two benchmarks, POPE and CHAIR, with the results presented in Tab.7. Our method continues to deliver significant performance improvements on a 13B model, indicating its strong generalizability. These results suggest

that our approach scales well and remains effective across different model sizes.

C.2 Divergence Between Images

Contrastive decoding is a method that suppresses consistent features between two distributions while amplifying distinctive ones. To prevent the loss of visual information during contrastive decoding, we select an image with sufficient discrepancy to construct a contrasting distribution. Thus, while maintaining language prior consistency, the divergent visual information helps avoid erroneous debiasing caused by feature overlap. We use CLIP to retrieve images based on cosine similarity, and select the image with the lowest similarity as the contrastive image. We conduct experiments to explore the correlation between similarity and performance, as shown in Fig. 7.

We observe that the similarity between images exhibits no strong correlation with performance. Compared to regular decoding methods, images with varying similarity levels all demonstrate significant improvements. As discussed in Sec.4.1, the influence of language priors is primarily reflected in the LVLMS’ comprehension of objects, attributes, and relationships. This information exhibits limited overlap across real-world images. We hypothesize that random image selection could achieve comparable effectiveness, with experimental results presented in Tab.8. Experimental results demonstrate that random image selection can also significantly mitigate language priors in LVLMS. In practical applications, the random selection approach offers greater convenience, substantially enhancing the usability of our method.

In Tab. 8, we also attempted to construct language priors by removing visual inputs, but found this approach less effective compared to eliminating linguistic priors through cross-image consistency. We attribute this limitation to LVLMS being trained on large-scale multimodal data, where re-

Method	Cs↓	Ci↓	Recall
	CHAIR(MaxLen=512)		
Regular	54.6	16.4	72.6
w/o Image	54.6	15.5	76.6
Random Image	46.6	13.2	76.7
Retrieved Image	43.8	11.7	75.0
Method	Cs↓	Ci↓	Recall
	CHAIR(MaxLen=64)		
Regular	24.4	8.9	56.6
w/o Image	25.4	7.6	61.9
Random Image	21.6	6.9	58.8
Retrieved Image	18.0	6.1	59.6

Table 8: This experiment was conducted by LLaVA-1.5. *Random Image* and *Retrieved Image* represent the contrastive images selected through random sampling and image retrieval, respectively. *w/o Image* represents the contrastive distribution that is constructed by removing the input image.

moving visual inputs disrupts the model’s intrinsic representations and leads to information distortion. Consequently, language priors in LVLMs cannot be directly constructed, which further substantiates the necessity of leveraging cross-image consistency in our method.

C.3 Threshold of Detrimental Priors

While language priors contribute to hallucinations in LVLMs, they also play a critical role in maintaining textual coherence and fluency. We employ JS divergence to distinguish between essential and detrimental priors, where essential priors exhibit high cross-image consistency, reflected in lower JS divergence scores. We establish a threshold of $\gamma = -4$ in Eq.6, based on the statistical distribution of JS divergence scores shown in Fig.6.

A comprehensive analysis is shown in Fig. 8. The experimental results align with the statistical analysis, demonstrating optimal performance at $\gamma = -4$. Another notable finding is that preserving essential priors proves meaningful, as it ensures fluent and coherent generation contexts.

D Analysis of Visual Information Overlap

Fig. 2 presents the overlap ratio of image-related words between responses generated from negative contexts and those from regular decoding. Below, we detail the analysis procedure.

First, we apply several contrastive decoding methods, each constructing its own negative con-

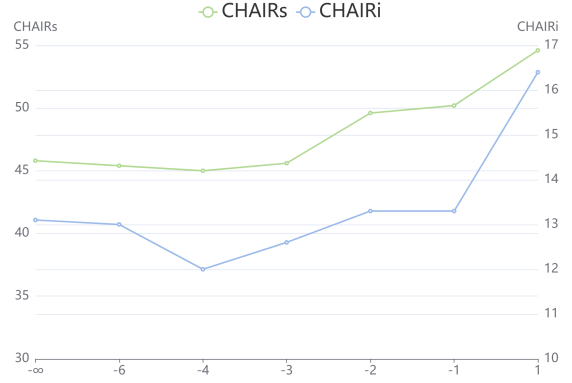


Figure 8: The results on the validation set of CHAIR using LLaVA-1.5. The X-axis represents the value of γ .

text, and use them to prompt LVLMs to answer user queries. For comparison, we obtain standard responses via regular decoding. We then use QwenVL-Max-0125 (Bai et al., 2023b) to extract image-related words from the generated responses. Inspired by CoT (Wei et al., 2022), we guide the model through a multi-stage extraction process: it first identifies all visually relevant words without access to the image, and then selects those strongly associated with the image content, which we define as *relevant words*.

Finally, we compute the overlap ratio between the relevant words generated from negative contexts and those obtained through regular decoding. This ratio quantifies how much essential visual content is preserved in responses generated from negative contexts, serving as an indicator of retained visual information. The prompt used to guide QwenVL-Max is shown in Fig. 9.

Based on this analysis, Fig. 2 shows that VCD and ICD retain over 30% of essential visual information, which is substantially weakened during contrastive decoding. In contrast, our method results in a negligible amount of residual information, effectively preventing visual information loss.

E Case Study

We present case studies to illustrate the superior performance of our method in hallucination reduction, as shown in Fig. 10 and Fig. 11. The image captions are generated by LLaVA-1.5. Red highlights indicate hallucinated content, while green highlights denote content consistent with the image.

We can clearly observe that Regular Decoding produces a substantial amount of hallucinated content, often manifesting as content words such as

objects, attributes, and relationships. In Fig. 10, for example, although the image depicts a skateboarding scene, the caption includes a reference to "spectators"—a detail not present in the image. Similarly, Fig. 11 shows an eating scene, yet the caption introduces a "long dining table," which is not actually visible. These hallucinations stem from LVLMs inheriting prior knowledge from LLMs, leading to biased descriptions in certain typical scenarios. In contrast, our method significantly reduces such hallucinations. While Fig. 11 still contains a hallucinated object (*chips*), this instance can be attributed to image ambiguity, where even human observers might plausibly infer such content.

Overall, our method effectively mitigates the influence of language priors by leveraging cross-image consistency.

Role

You are an image-understanding specialist who thoroughly comprehends visual content.

Task

You will receive an image together with a piece of caption text that describes it. The text is produced by a large language model and may contain words that do ****not**** correspond to the image (hallucinated content).

Follow the steps below.

1 · Identify **Visual Words**

- Strictly ignoring the provided image, select every word from the caption text that refers to a visual concept, to form the Visual Words list.
- Typical examples include objects, colours, shapes, poses, scenes, quantities and text visible in the picture.

2 · Filter **Relevant Words**

- From the Visual Word set keep only those words that accurately match the provided image and can be verified objectively.
- Discard conjecture, emotion, narrative and any subjective judgement.

3 · Output

- Return a JSON object containing two lists, "Visual Word" and "Relevant Word", each holding the raw words you extracted.
- Preserve every word's original casing and punctuation.

Input

Caption text: {caption_text}

Output format

```
```json
{
 "Visual Word": ["word1", "word2", ...],
 "Relevant Word": ["wordA", "wordB", ...]
}
```

### ### Guidelines

- Ensure the Relevant Word list contains only those words that can be objectively confirmed in the provided image.
- Follow the output format exactly.

Figure 9: Prompt for guiding QwenVL-Max to progressively extract relevant words from the response.





#### Regular

In the image, there is a **young man** skillfully riding a skateboard up the side of a **cement skateboard ramp**. He is dressed casually, with a white shirt and **no shoes**. **Another person can be seen standing near the top of the ramp, possibly waiting for their turn or watching the skateboarder perform the stunt**. In addition to the skateboarder and passer-by, there is **another skateboard** present in the scene, likely belonging to the young man riding up the ramp. There is a **chair** parked near the skateboard ramp, and numerous potted **plants** are scattered throughout the scene, adding a sense of the outdoor environment.

#### CICD

The image captures a **young skateboarder** skillfully riding up the side of a **cement skateboard ramp**. The **boy** is performing a trick, jumping high on the skateboard and momentarily taking off from the ramp. He is wearing a **helmet** for safety, and there is a **chair** in the background on the **right** side of the scene. The surrounding area features **trees** and **flowers**, adding a vibrant and lively atmosphere to the scene. There are at least five **trees** visible in various positions around the skateboarder, with some closer and others further in the background.

Figure 10: Case study (1).



#### Regular

The image shows a group of **people** sitting on brightly colored **chairs** around a **dining style long table**. The **table** is filled with numerous **drink bottles, cups, and snacks**, such as **donuts**, indicating that the gathering might be a party or a social event. There is a diverse array of individuals present, and some of them appear to be **young**. A **toddler** has been joined by an older **gentleman** at the table, creating a lively atmosphere. The guests are engaged in various activities, either enjoying the party or mingling with each other. Near the table, there is a **laptop**, suggesting the event may have digital components or multimedia. In addition to the main table area, a **backpack** is present in the scene, indicating that someone may have left it behind, or it could be a part of an impromptu meeting.

#### CICD

In this scene, several **adults** and **children** are gathered in a **classroom**, engaged in conversation. Some of the adults appear to be politicians, while others may be teachers, parents, or guardians. A politician can be seen **smiling** as he **sits** among the children at their table, eating food like **apples, milk, and chips**. There are numerous **chairs, desks, and tables** scattered throughout the **classroom**, indicating a **learning** environment. Various items are also present in the room, including **books, bottles, apples, cups, and a TV**. A backpack is placed near the edge of the room. The atmosphere in the classroom seems to be casual and friendly, with both children and adults participating in a dialogue, sharing food and drinks, and enjoying each other's company.

Figure 11: Case study (2).